

Supplemental material

Vion et al., <https://doi.org/10.1083/jcb.201706151>

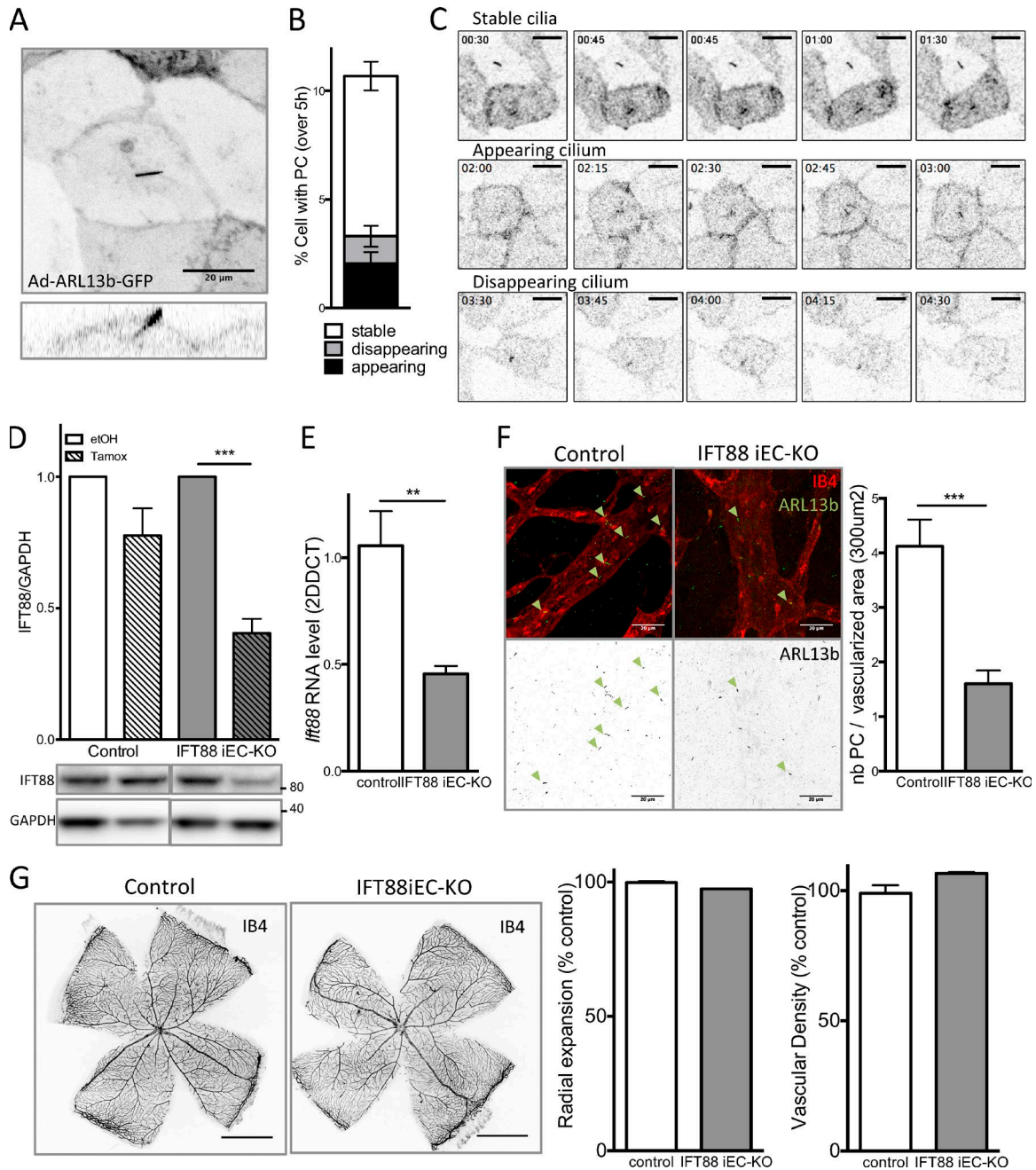


Figure S1. **Dynamics of endothelial cilia in vitro and validation of the mice model.** (A) HUVEC infected with adenovirus encoding for ARL13b-GFP. The first image shows a z-projection of a ciliated cell; the second image shows a section showing the cilium protruding on the luminal side (observed on five biological replicates). (B) Quantification of ciliated cells that remain stable, disappear, or appear over time (5 h, two biological replicates, 10 technical replicates; mean \pm SEM). (C) Stills extracted from Video 4 showing stable cilia (top), formation of a cilium (middle), or retraction of a cilium (bottom). The images were acquired using an open pinhole avoiding loss of focus. Bars, 20 μ m. (D) Western blot analysis for IFT88 was performed on lung ECs extracted from IFT88 iEC-KO mice and littermate controls treated either with DMSO (plain white and gray) or with 1 μ mol/l tamoxifen (hatched white and gray) for 120 h ($n = 3$, mean \pm SEM; two-sided paired t test; ***, $P < 0.001$). Molecular masses are indicated on the images based on prestained protein standard. (E) *Ift88* RNA levels were quantified by quantitative PCR in retinal ECs extracted from IFT88 iEC-KO mice and littermate controls ($n = 7$, mean \pm SEM; two-sided Wilcoxon test; ***, $P < 0.001$). (F) Eyes from IFT88 iEC-KO mice and littermate controls were collected at P6 and stained for ARL13b (primary cilia, green) and with Isolectin B4 (IB4, red). The number of ECs showing PC (green arrowheads) was quantified in both groups ($n = 5$, median \pm IQ; two-sided Wilcoxon test; ***, $P < 0.001$). Bars, 20 μ m. (G) Eyes from IFT88 iEC-KO mice and littermate controls were collected at P15 and stained with Isolectin B4 (black). Radial expansion and vascular density were quantified in both groups (WT, $n = 3$; KO, $n = 3$; median \pm IQ). Bars, 1,000 μ m.

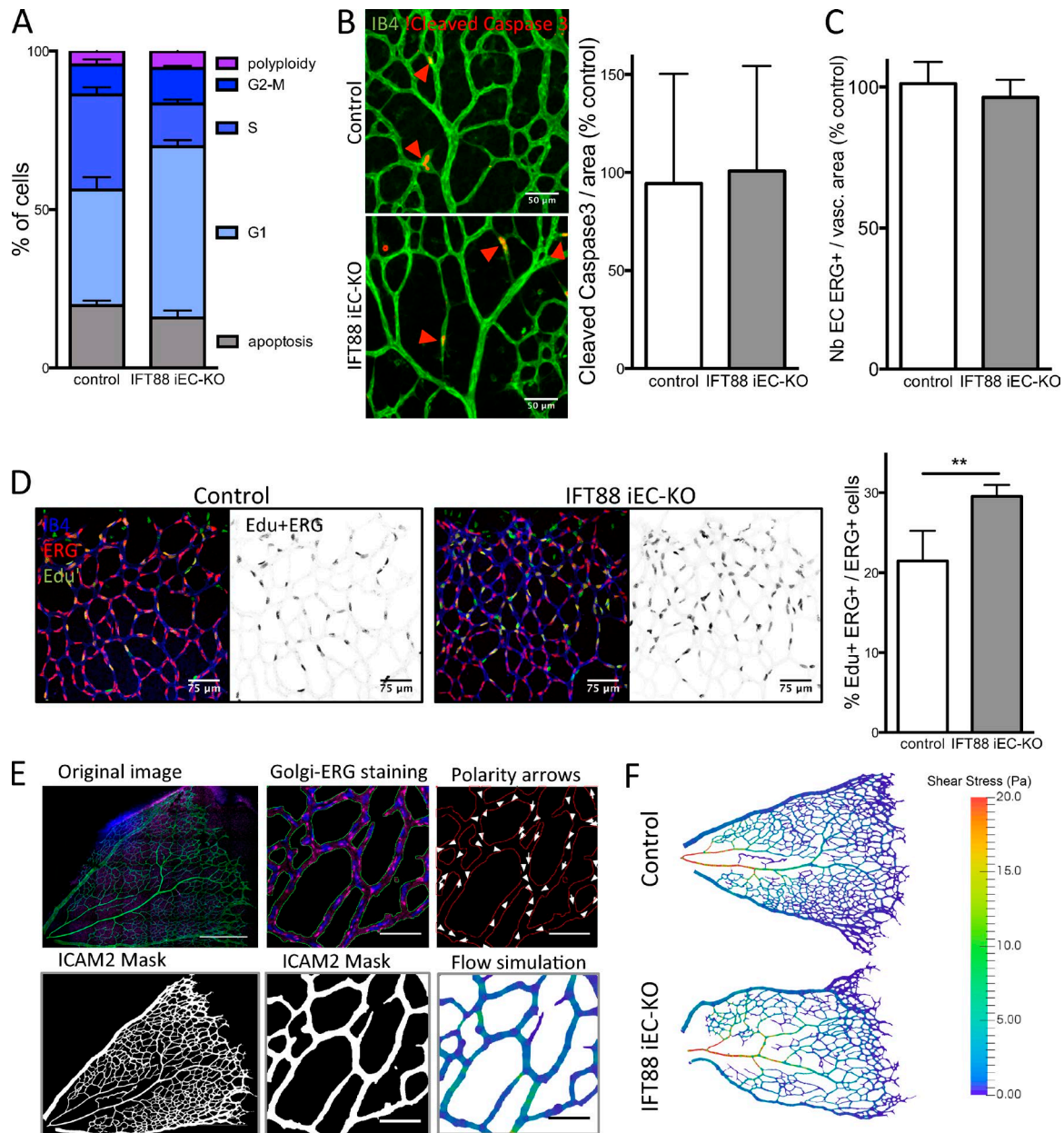


Figure S2. IFT88 iEC-KO mice reduced vascular density is not dependent on cell cycle of ECs. (A) The proportion of ECs in each phase of the cell cycle was assessed by flow cytometry analysis of retinal ECs extracted from IFT88 iEC-KO retinas and littermate controls at P6 (WT, $n = 4$; KO, $n = 8$; median \pm IQ). (B) Retinas from P6 IFT88 iEC-KO and littermate control mice were stained for cleaved caspase-3 (red) and with Isolectin B4 (green). Red arrowheads indicate apoptotic ECs. The number of ECs undergoing apoptosis per vascular area was quantified in both groups ($n = 8$; median \pm IQ). Bars, 50 μ m. (C) The number of ECs per vascular area was quantified in retinas of IFT88 iEC-KO and littermate control mice stained for ERG (endothelial nuclei) and with Isolectin B4 at P6 (WT, $n = 8$; KO, $n = 10$; median \pm IQ). (D) IFT88 iEC-KO and littermate control mice were injected with EdU at P6. Eyes were collected after 2 h and retinas were stained for EdU (green) or ERG (red) and with Isolectin B4 (blue). Bottom panels show ERG⁺/EdU⁺ nuclei corresponding to proliferating ECs. The proportion of ECs undergoing proliferation was quantified in both groups (WT, $n = 6$; KO, $n = 7$; median \pm IQ; two-sided Wilcoxon test; **, $P < 0.01$). Bars, 75 μ m. (E) IFT88 iEC-KO and control retinas were processed for Polnet analysis. The upper-left image shows the original image acquired (green, ICAM2; red, GOL PH4 [Golgi]; blue, ERG), from which a mask was generated based on the ICAM2 staining to show only lumenised vessels (bottom-left image). Bars, 400 μ m. Top and bottom-middle images show high magnification images of the Golgi-ERG staining used to measure polarity and the corresponding ICAM2 mask, respectively; Bars, 50 μ m. The top-right image shows the polarity arrows (white arrows) drawn based on the upper-middle image. The bottom-right image shows the corresponding flow simulation. Bars, 50 μ m. (F) Flow simulation was performed in both IFT88 iEC-KO retinas and littermate controls. Images are representative of three independent animals.

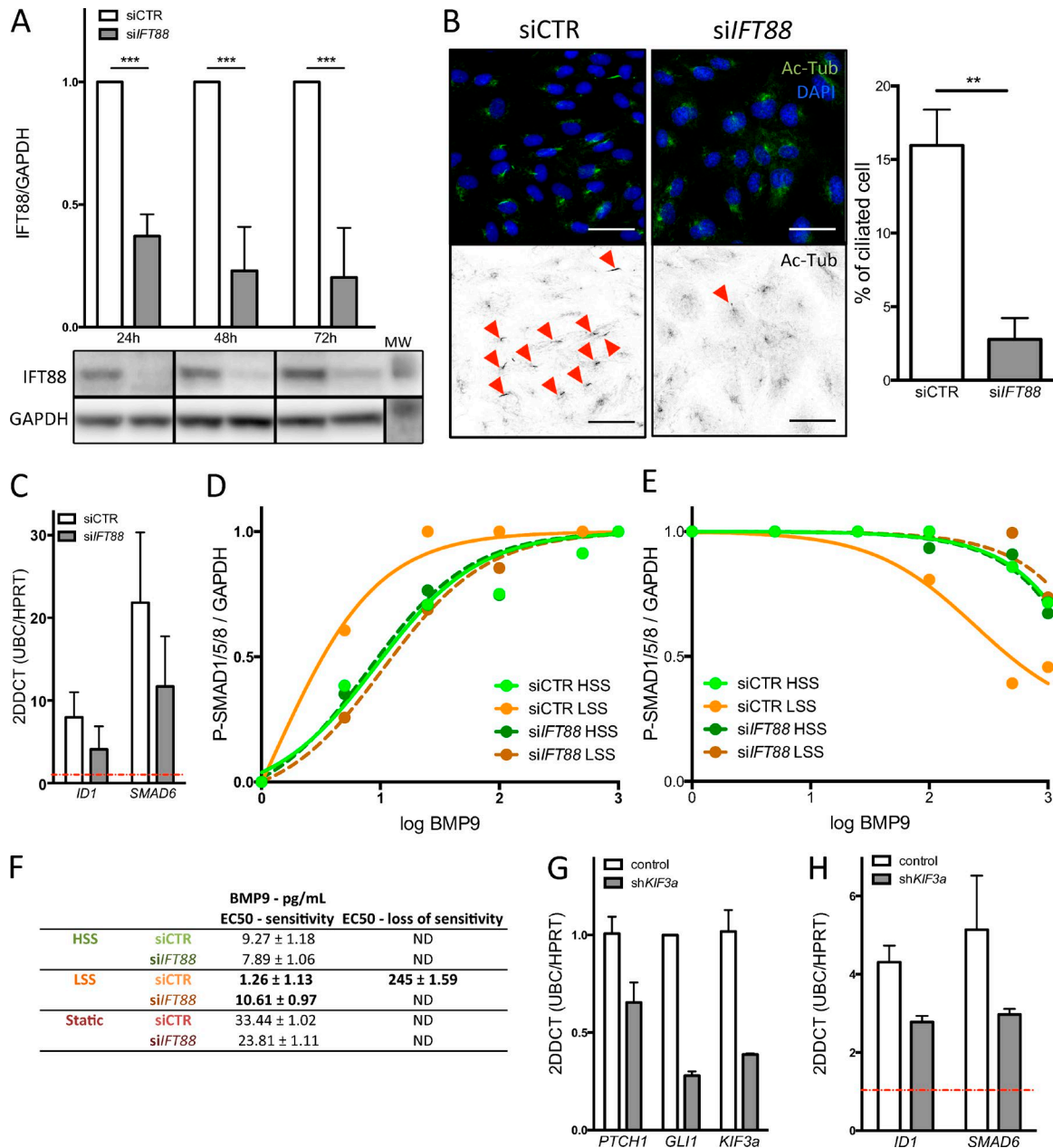
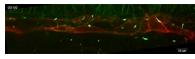
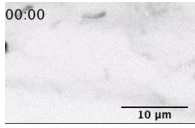


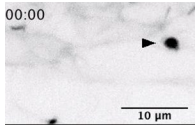
Figure S3. Loss of the primary cilium blocks the differential response to BMP9 under flow in vitro. (A) The efficiency of IFT88 silencing in HUVECs using siRNAs was evaluated by Western blot analysis (white, siCTR; gray, siIFT88; $n = 5$, mean \pm SEM; two-sided Wilcoxon test; ***, $P < 0.001$). MW on the IFT88: 80kD; MW on the GAPDH: 40kD (from the bright field image). (B) The percentage of cells with primary cilia was quantified after IFT88 silencing using immunostaining for DAPI (blue) and acetylated tubulin (Ac-Tub, green) 48 h after transfection ($n = 5$, mean \pm SEM; two-sided Wilcoxon test; **, $P < 0.01$). Red arrowheads point at primary cilium. Bars, 40 μ m. (C) Quantitative PCR analysis of BMP9 target genes was performed in siCTR (white) and siIFT88 transfected cells (gray) upon BMP9 stimulation (25 pg/ml, 2-h treatment; $n = 3$; mean \pm SEM). (D) Dose-response fitting curves used for determining the EC50 for sensitivity to BMP9 in siIFT88 and siCTR transfected ECs ($n = 3$; mean only). (E) Dose-response fitting curves used for determining the EC50 for loss of sensitivity to BMP9 in siIFT88 and siCTR transfected ECs ($n = 3$; mean only). (F) Table with the EC50 values for each condition. (G) Quantitative PCR analysis of *PTCH1*, *GLI1*, and *KIF3a* was performed in shCTR- (white) and sh*KIF3a*-infected cells (gray; $n = 3$; mean \pm SEM). (H) Quantitative PCR analysis of BMP9 target genes was performed in shCTR- (white) and sh*KIF3a*-infected cells (gray) upon BMP9 stimulation (25 pg/ml, 2-h treatment; $n = 3$; mean \pm SEM). ND, not determined.



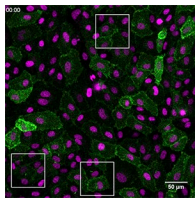
Video 1. **Endothelial cilia are luminal and dynamic in zebrafish embryo.** Representative movie of the aorta of a Tg(kdr-l:ras-Cherrys916; β -actin::arl13b-eGfp) zebrafish embryo imaged at 24 h after fertilization (time frame, 5 min) for 6 h (representative of two fish). Red, EC membrane labeling; green, ARL13b-GFP-cilium labeling.



Video 2. **Endothelial cilium formation in zebrafish embryo.** Representative movie of an endothelial cilium forming over 6 h of imaging. Black, ARL13b-GFP-cilium labeling. The cilium localization is indicated with a star in the movie and presented as stills in Fig. 1 F (representative of two fish and three cilia).



Video 3. **Endothelial cilium retraction in zebrafish embryo.** Representative movie of an endothelial cilium retracting over 6 h of imaging. Black, ARL13b-GFP-cilium labeling. The cilium localization is indicated with an arrowhead in the movie and presented as stills in Fig. 1 F (representative of two fish and four cilia).



Video 4. **Endothelial cilia dynamics in vitro.** Representative movie of cilia dynamics observed using an adenovirus encoding for ARL13b-GFP. Green, ARL13b-GFP; magenta, nuclei. Representative of two biological replicates and ten technical replicates. White squares indicate the positions taken for the stills of Fig. S1 C.